



# Nanosized charge-transfer salts of metal phthalocyanine iodides ([MPc]I) produced by direct reaction of MPc-silica hybrid nanoparticles with iodine

Funabiki, Akira  
Mochida, Tomoyuki  
Hasegawa, Hiroyuki  
Ichimura, Kunihiro  
Kimura, Seiji

---

(Citation)

New Journal of Chemistry, 35:483-488

(Issue Date)

2011

(Resource Type)

journal article

(Version)

Accepted Manuscript

(URL)

<https://hdl.handle.net/20.500.14094/90001803>



# **Nanosized charge-transfer salts of metal phthalocyanine iodides ([MPc]I) produced by direct reaction of MPc–Silica hybrid nanoparticles with iodine**

**Akira Funabiki,<sup>a</sup> Tomoyuki Mochida,<sup>\*,a</sup> Hiroyuki Hasegawa,<sup>b,c</sup> Kunihiro Ichimura,<sup>d</sup> and Seiji Kimura<sup>e</sup>**

<sup>a</sup>*Department of Chemistry, Graduate School of Science, Kobe University, Kobe, Hyogo 657-8501, Japan. E-mail: tmochida@platinum.kobe-u.ac.jp*

<sup>b</sup>*Kobe Advanced ICT Research Center, National Institute of Information and Communications Technology, Kobe, Hyogo 651-2492, Japan*

<sup>c</sup>*PRESTO, Japan Science and Technology Agency, Kawaguchi, Saitama 332-0012, Japan*

<sup>d</sup>*Faculty of Science, Toho University, Funabashi, Chiba 274-8510, Japan*

<sup>e</sup>*The University of Electro-Communications, Chofu, Tokyo 182-8585, Japan*

## **Summary:**

An efficient preparation of nanosized charge-transfer (CT) salts of metal phthalocyanine iodides has been achieved by direct reaction of metal phthalocyanine–silica hybrid nanoparticles with iodine. The direct reaction was enabled by the enhanced reactivity of the nanoparticles, which possess enlarged surface areas. TEM observation revealed that the [MPc]I salts thus formed separate from the shell layers of the nanoparticles during reaction to form rod-shaped nanostructures of hundreds of nanometers in length and about 30 nm in diameter.

## Introduction

Nanoparticles of metals, semiconductors and organic compounds have been attracting ever increasing research interest.<sup>1</sup> The nano-downsizing of solids affects their physical and chemical properties due to a remarkable increase in the proportion of surface atoms or molecules as well as due to quantum effects, leading to unique properties different from those of the bulk solids.<sup>1</sup> Charge-transfer (CT) salts composed of organic donors and acceptors exhibit a variety of physical properties such as electrical conductivity, magnetism, phase transitions and so forth.<sup>2</sup> The nano-downsizing of CT salts is an attractive research target because their electronic properties are sensitive to external stimuli, and thus size effects are anticipated to play crucial roles in determining their physical properties. In addition, fabrication of 2D and 3D nanostructured assemblies has received remarkable attention in terms of its potential for construction of nanoscale electronic and optical devices,<sup>3a-c</sup> and CT salts are interesting in this respect as well.<sup>3d, 4</sup> A few fabrication techniques for preparing fine crystals of CT complexes reported to date include electrolysis<sup>4</sup>, vapor deposition<sup>5</sup> and reprecipitation.<sup>6</sup>

Organic nanocrystals of sizes ranging from a few tens of nanometers to sub-micrometers have been fabricated by reprecipitation<sup>7</sup> and laser ablation<sup>8</sup> to give dispersions in poor solvents. With regard to smaller hybrid nanomaterials, it has recently been reported that mechanical grinding of organic pigments including metal phthalocyanines (MPc)<sup>9</sup> and molecular crystals<sup>10</sup> in the presence of silica nanoparticles affords core-shell type hybrid nanoparticles. Energy-filtered transmission electron microscope observations revealed that the surfaces of the aggregated primary nanoparticles of silica are covered with organic shell layers a few nanometers in thickness, while a fraction of the pigments densely fill in hollow spaces at the joint sites of the aggregated primary silica particles.<sup>9b</sup> The nanohybridization with silica nanoparticles leads to a notable increase in the surface area of the organic material, and surface-specific photochemical as well as physicochemical behaviors have

been elucidated.<sup>10</sup> For example, the BET (Brunauer-Emmett-Teller) specific surface area of a 1:1 (w/w) hybrid of CuPc and silica nanoparticles is 86.6 m<sup>2</sup>/g.<sup>9b</sup> Such a large surface area is highly preferable for reactions in the solid state. Organic solid state reactions have received much attention<sup>11</sup> because of their simplicity and specific reactivity. In solid state reactions, major emphasis is placed on mechanochemical effects. The use of the hybrid nanoparticles is advantageous for exploring the surface effects in solid state reactions and for the fabrication of secondary nanostructures.

In the current study, metal phthalocyanines (MPc) (M = Cu, Ni) were selected for the preparation of CT salts using the silica hybrid nanoparticles. CT salts of MPc are familiar as electrically conductive materials.<sup>12-14</sup> In [MPc]I (Fig. 1), which are prepared by partial oxidization of MPc with iodine, MPc molecules are stacked to form conduction columns.<sup>13,14</sup> We report herein the reaction of solid MPc (M = Ni, Cu) in the shell layers of the hybrid nanoparticles with iodine to quantitatively produce [MPc]I. The high reactivity of the hybridized MPc is notable, considering the low reactivity of bulk MPc. The rod-shaped nanostructures of the resultant CT salts were also interesting. Overall, core-shell hybrid nanoparticles were shown to be useful for efficiently producing molecular complexes that may exhibit novel nanostructures and functions.

## Results and discussion

### Preparation of MPc-silica hybrid nanoparticles

MPc-silica hybrid nanoparticles were fabricated according to the reported procedure<sup>10</sup> by grinding a 1:1 (w/w) mixture of NiPc and the surface-modified silica nanoparticles (14.1 nm diameter for primary particles) using nylon beads in a table-top planetary mill to give blue powders. The surface of the silica nanoparticles was modified with methylhydrogenpolysiloxane in advance to reduce the surface polarity of the powder and thus improve the affinity of the silica surfaces for the MPc. The

powdery composites were subjected to X-ray diffraction (XRD) analysis to characterize the structures of the hybridized MPc. As can be seen in Fig. 2b, the diffraction peaks of the original NiPc (Fig. 2a) were considerably reduced and broadened, suggesting transformation to an amorphous state or pronounced reduction of crystallite sizes. The diffraction peak at  $2\theta = 6.98^\circ$  corresponding to the stacking axis (*c*-axis) of the unit cell is retained, implying that the short-range order is preserved after hybridization. A hybridized blue powder of a 1:1 (w/w) mixture of CuPc and silica nanoparticles obtained under the same grinding conditions yielded very similar XRD results (Fig. 2c). The MPc hybrid nanoparticles showed aggregated structures of spherical primary particles (Fig. S3).

The IR stretching frequency for the out-of-plane C–H bending mode ( $\gamma_{\text{CH}}$ ) in MPc crystals is known to be dependent on the crystal form.<sup>15</sup> While CuPc in the  $\beta$ -form, which was used as the starting material, exhibited a  $\gamma_{\text{CH}}$  at  $730\text{ cm}^{-1}$ , the  $\gamma_{\text{CH}}$  of the CuPc–silica composite nanoparticles appeared at  $725\text{ cm}^{-1}$ , suggesting that the microenvironment of the CuPc in the nanoparticles resembled that of the  $\alpha$ -form, which shows a  $\gamma_{\text{CH}}$  at  $725\text{ cm}^{-1}$  (Fig. S1).<sup>15</sup> This shift implies transformation of the crystal microenvironment. Annealing of the as-milled CuPc nanocomposite powder at  $250^\circ\text{C}$  resulted in the growth and narrowing of the XRD diffraction peaks ascribable to the  $\beta$ -form, suggesting that crystal growth occurred, to produce the most thermally stable  $\beta$ -form (Fig. 2d). The transformation was also confirmed by the appearance of a  $\gamma_{\text{CH}}$  at  $730\text{ cm}^{-1}$  in the FT-IR spectra.

### **Reaction of hybrid nanoparticles with iodine**

The complexation of the nanohybrids with iodine was achieved under both dry and wet conditions. Firstly, the NiPc nanohybrid powder was ground for 1 hr with an equimolar amount of iodine using nylon beads. The blue powder turned black after the grinding, and the quantitative 1:1 complexation was confirmed by the absence of iodine color in hexane washings. The XRD pattern of the as-prepared 1:1 salt of NiPc with iodine ([NiPc]I) shown in Fig. 3a indicates only slight modification

when compared with that of the NiPc hybrid. In contrast, the diffraction peaks due to [NiPc]I grew after washing with hexane (Fig. 3b). It is likely that either the mobility of the molecules is enhanced via solvation or the complexation of an unreacted portion was induced by the solvent, but the majority of the salt in the composite was amorphous (vide infra) and only a minor portion gave rise to the diffraction peaks. The crystalline size of the component was remarkably small ( $< 20$  nm) as estimated by Scherrer's equation. Washing with water did not affect the XRD pattern. CuPc also formed an amorphous iodide salt under similar conditions. The resultant [CuPc]I nanocomposite was stable at ambient temperature, while slight elimination of iodine was observed under reduced pressure. Annealing at  $250\text{ }^{\circ}\text{C}$  caused complete elimination of iodine, yielding blue colored CuPc, which was confirmed by XRD measurements.

The reaction with iodine was also conducted under wet conditions by dissolving an equimolar amount of iodine into a stirred dispersion of NiPc composite nanoparticles in hexane. The color of the iodine disappeared thoroughly, indicating that the reaction occurred stoichiometrically. The black powder thus formed showed an XRD pattern corresponding to that of [NiPc]I with weak intensities (Fig. 3c) and closely resembling that of the solid-doped sample after washing (Fig. 3b). These results indicate that the growth of the crystalline component is associated with the use of hexane, which dissolves the iodine. The XRD pattern of the CuPc composite powder after the reaction with iodine in hexane indicated the presence of a small percentage of original CuPc, suggesting a slightly lower reactivity of CuPc with iodine. These results indicate that the use of MPc–silica hybrid nanoparticles enables direct reaction with iodine without prior dissolution of MPc. Typically, [MPc]I salts are synthesized by a diffusion method using solvents such as 1-chloronaphthalene.<sup>12-14</sup>

To examine the effect of the downsizing of MPc to the nanoscale, the dry grinding of a mixture of MPc ( $M = \text{Cu, Ni}$ ) and an equivalent amount of iodine was carried out in the absence of silica nanoparticles. This procedure afforded bluish to black powders, but the XRD analysis showed that they were predominantly comprised of a mixture of unreacted MPc and  $\text{I}_2$ . These results confirmed

the significant role of the hybridization with the silica nanoparticles, which resulted in extremely enlarged surface areas and probably also modification of the molecular arrangement in the MPc crystals that led more or less to higher reactivity. It is important to note that this reaction method can be applied to the reaction of compounds that are insoluble in solvents or that are less reactive in the solid state.

### **Electron microscopy**

A TEM image of NiPc–silica composite nanoparticles reacted with iodine under dry conditions is shown in Fig. 4, which reveals the formation of rod-like nanostructures of about 30 nm in diameter. The rod-shaped nanostructures were also observed for the [CuPc]I–silica nanocomposite. In all of the samples, the nanorods were bundled and accompanied by particles that adhered to them, as can be seen in Fig. 4a. Noting that MPc hybrid nanoparticles before reaction with iodine showed aggregated structures of spherical primary particles and that the rod-like nanostructures are observed before and after washing, it is reasonable to conclude that the nanorods are formed and grown during the reaction with iodine. The same characteristic nanostructures were also observed for samples obtained under wet conditions (Fig. 5). Fig. 5a is an SEM image of a highly aggregated structure.

Energy dispersive X-ray spectroscopy (EDX) analysis was performed to reveal the elemental distribution of the nanorods (Fig. 6 and Fig. S4). In Fig. 6, Si from silica is detected only in the lower right portion of the image, and the nanorods exhibited the presence of C, N, Ni, and I, indicating unequivocally that the nanorods consisted of [NiPc]I and were free from silica particles. Silica nanoparticles mainly existed as aggregated particles and can be seen as white objects in Fig. 5a. Electron diffraction patterns of the nanorods showed halo rings (Fig. S5), indicating their amorphous nature. Although they were not crystalline, short-range order may be retained due to the stacked structure of the [MPc]I molecules in the bulk crystals. While the washing of samples prepared under dry conditions with hexane led to a slight growth of crystalline components as described above, this

sort of crystalline component may be so small in size, and probably located in aggregated structures,<sup>9b</sup> that they were not observed by electron microscopy.

The mechanism of formation of the nanorods of [MPc]I is of interest. The MPc molecules in the hybrid nanoparticles are converted into cations upon reaction with iodine, and separation from the silica nanoparticles occurs probably due to their reduced affinity to the hydrophobic silica surfaces. Consequently, the MPc molecules likely favor self-aggregation as the salts, and the stacking tendency of the planar molecule probably leads to growth of the rod-like structures. The large and flat molecular shape of MPc may be responsible for the smaller affinity of the cation with the silica surface, because the affinity seems to be affected by the spherical curvature of the silica nanoparticles.<sup>16</sup> The tendency of MPc salts to form one-dimensional assembled-structures may be an additional factor favoring the removal from the silica surface. Indeed, we also applied the same procedure to BEDT-TTF (= bis(ethylenedithio)tetrathiafulvalene), which similarly gives CT salts by reaction with iodine, to find that only core-shell nanoparticles of the iodide were produced.<sup>17</sup> BEDT-TTF is a smaller, more flexible molecule than MPc that favors two-dimensional assembled structures. This comparison indicates that nanostructures produced by the present method strongly depend on the properties of the constituent molecules. In the [MPc]I–silica nanocomposite, silica nanoparticles are adhered around the nanorods. Interestingly, the composite powders disperse rather well in organic solvents, which may be partly due to the presence of the hydrophobically surface-modified silica. Increased dispersibility in hydrophobic matrices of organic solvents and polymers is advantageous for various applications.

### **Electrical conductivity**

FTIR spectra of [MPc]I–silica nanocomposites showed broad absorption bands characteristic of electrical conductors. Electrical conductivities of compacted pellets of the powder samples were measured at room temperature. The MPc–silica composite nanoparticles were complete insulators (<



$10^{-10} \text{ S cm}^{-1}$ ) before reaction with iodine, while [CuPc]I–silica nanocomposites prepared under wet conditions exhibited conductivity of ca.  $2 \times 10^{-6} \text{ S cm}^{-1}$ . The conductivity was thus increased by the formation of CT salts, but was much lower than that of the bulk crystals of [MPc]I ( $\sim 10^3 \text{ S cm}^{-1}$ ).<sup>12</sup> The very low conductivity is attributed to the amorphous nature of the [MPc]I nanorods, the existence of silica nanoparticles, and the presence of a large number of grain boundaries due to the nanostructures. An attempt to remove silica nanoparticles by an alkaline treatment lead to decomposition of the CT salts. Electrical conductivities of [NiPc]I–silica nanocomposites were not measured because the preparation of pellets was difficult, while they may be similar to that of [CuPc]I–silica nanocomposites considering their close similarities. Direct measurements of the conductivity of the nanorods using a scanning probe microscope were unsuccessful because of their extremely small size and aggregated structures.

## Conclusions

MPc–silica hybrid nanoparticles fabricated via grinding produced CT salts of [MPc]I through a direct reaction with iodine. The composite powder was found to be structurally interesting; the CT salt separated from the silica surface to form rod-like nanostructures with diameters of about 30 nm. The remarkably enhanced reactivity of MPc is notable, since iodine doping of bulk MPc in the solid state does not occur efficiently. The use of silica hybrid nanoparticles as presented here is a simple, novel and highly productive method due to the high reactivity of the surface molecules. The higher reactivity enables more efficient processes than conventional solid state reactions, and may even enable the use of poorly-soluble compounds. In addition, while conventional investigation of CT salts has focused predominately on single crystals or films, access to nanosized composite materials expands the scope and applications of these complexes. For example, their nanosize may lead to unusual physical properties, while the high dispersibility of nanosized materials in liquids is

advantageous for various applications.<sup>18</sup> Furthermore, the efficiency as well as the simplicity of the present method is of merit for large scale production of functional nanomaterials. Exploration of the functionalities and nanostructures of various molecular complexes prepared with the present method is therefore of further interest.

## Experimental

### Materials

The surface of Stöber silica nanoparticles (Toso Silica; NIPSIL VN3, primary particle diameter of 14.1 nm) was modified with methylhydrogenpolysiloxane to reduce the surface polarity of the powder so as to improve the affinity of the silica surfaces for the MPc. The surface-modified silica powders were gifted by Toda Kogyo Co., Ltd. Metal phthalocyanines (MPc, M = Cu, Ni) in the  $\beta$ -form were purchased from Wako and Strem, respectively, and sublimed prior to use.

### General

XRD data for the powders was recorded on a Rigaku SmartLab diffractometer using Cu  $K\alpha$  radiation. Electron micrographs were obtained using a JEOL JEM-2010 TEM and a JEOL JSM-6700F field emission scanning electron microscope (FE-SEM). Specimens for TEM observation were prepared by dropping an aqueous dispersion of a powdery sample on a copper grid supported with a carbon membrane followed by drying in vacuo at ambient temperature. FE-SEM observations were carried out on a silicon wafer spin-coated with an aqueous dispersion of the powdery samples. FT-IR spectra were recorded on a Perkin Elmer Spectrum 1000 spectrometer using KBr plates. For conductivity measurements, powdery samples were pressed into pellets under a pressure of 500 kg cm<sup>-2</sup> by using a hydraulic molding press. Conductivity was measured by the ac impedance technique at ambient temperature with an applied voltage of 1 V using a Solartron 1260 impedance analyzer. XRD

patterns were simulated using Mercury CSD software (v. 2.3) available from Cambridge Crystallographic Data Centre.

### **Preparation of [MPc]I–silica nanocomposites**

MPc–silica composite nanoparticles were fabricated according to the method reported in the literature.<sup>10</sup> Silica nanoparticles (100 mg) and a desired amount of MPc were placed in zirconia vessels (12 mL) and milled with the aid of nylon beads in a Fritsch P-7 planetary mill at 400 rpm for 1 h. The obtained composite nanoparticles and an equimolar amount of iodine were then milled, also with the aid of nylon beads. The resulting powders were washed with hexane (2 mL) and the supernatant was removed with aid of a centrifuge. The washing was repeated three times, and the powders were dried in vacuo at room temperature. Alternatively, the reaction with iodine was carried out under wet conditions as follows. To MPc–silica composite nanoparticles dispersed in a hexane solution was dissolved an equimolar amount of iodine, and the resulting dispersion stirred for 3 h. The supernatant was separated with aid of a centrifuge, and the resulting powders washed in a manner similar to the procedure stated above and then dried in vacuo at room temperature.

### **Acknowledgments**

We thank Prof. D. Kuwahara (The University of Electro-communications) for his help with the instrumental analyses and Prof. T. Uchino (Kobe University) for his support throughout this work.

Electronic Supplementary Information (ESI) available: SEM images of CuPc–silica hybrid nanoparticles and an EDX spectrum of [NiPc]I nanorods.

## References

- (1) (a) G. Schmid, Eds. *Nanoparticles: From Theory to Application*; Wiley-VCH, 2004; G. Cao, Eds. *Nanostructures & Nanomaterials : synthesis, properties & applications*; Imperial College Press: London, 2004; H. S. Nalwa, *Nanostructured Materials and Nanotechnology*; Academic Press: New York, 2002; A. P. Alivisatos, *Science* 1996, **271**, 933–937.
- (2) Special issue, *Chem. Rev.* 2004, **104**; Special issue, *J. Phys. Soc, Jpn.* 2006, **75**; T. Ishiguro, K. Yamaji, G. Saito, *Organic superconductors* 2nd Ed.; Springer-Verlag: Berlin, 1998.
- (3) M. S. Gudiksen, L. J. Lauhon, J. Wang, D. C. Smith, C. M. Lieber, *Nature* 2002, **415**, 617–620; J. S. Jung, J. W. Lee, K. Kim, M. Y. Cho, S. G. Jo, J. Joo, *Chem. Mater.* 2010, **22**, 2219–2225; S. Takami, Y. Shirai, Y. Wakayama, T. Chikyow, *J. Mater. Chem.* 2008, **18**, 4347–4350; K. Tanaka, T. Kunita, F. Ishiguro, K. Naka, Y. Chujo, *Langmuir* 2009, **25**, 6929–6933.
- (4) H. Hasegawa, T. Kubota, S. Mashiko, *Thin Solid Films* 2003, **438–439**, 352–355; H. Hasegawa, Y. Noguchi, R. Ueda, T. Kubota, S. Mashiko, *Thin Solid Films* 2008, **516**, 2491–2494; H. M. Yamamoto, H. Ito, K. Shigeto, K. Tsukagoshi, R. Kato, *J. Am. Chem. Soc.* 2006, **128**, 700–701.
- (5) K. Xiao, I. N. Ivanov, A. A. Puztzky, Z. Liu, D. B. Geohegan, *Adv. Mater.* 2006, **18**, 2184–2188. K. Xiao, J. Tao, Z. Pan, A. A. Puztzky, I. N. Ivanov, S. J. Pennycook, D. B. Geohegan, *Angew. Chem. Int. Ed.* 2007, **46**, 2650–2654.
- (6) K. Hiraishi, A. Masuhara, T. Yokoyama, H. Kasai, H. Nakanishi, H. Oikawa, *J. Cryst. Growth* 2009, **311**, 948–952; K. Hiraishi, A. Masuhara, H. Kasai, H. Nakanishi, H. Oikawa, *Jpn. J. Appl. Phys.* 2010, **49**, 01AE08.
- (7) H. Kasai, H. S. Nalwa, H. Oikawa, S. Okada, H. Matsuda, N. Minami, A. Kakuta, K. Ono, A. Mukoh, H. Nakanishi, *Jpn. J. Appl. Phys.* 1992, **31**, L1132–L1134.
- (8) T. Asahi, T. Sugiyama, H. Masuhara, *Acc. Chem. Res.* 2008, **41**, 1790–1798.

- (9) K. Hayashi, H. Morii, K. Iwasaki, S. Horie, N. Horiishi, K. Ichimura, *J. Mater. Chem.* 2007, **17**, 527–530; S. Horiuchi, S. Horie, K. Ichimura, *ACS Appl. Mater. Interfaces* 2009, **1**, 977–981
- (10) K. Ichimura, *Chem. Comm.* 2010, **46**, 3295–3297; K. Ichimura, A. Funabiki, K. Aoki, *Chem. Lett.* 2010, **39**, 586–587; K. Ichimura, K. Aoki, H. Akiyama, S. Horiuchi, S. Nagano, S. Horie, *J. Mater. Chem.* 2010, **20**, 4312–4320; K. Ichimura, K. Aoki, H. Akiyama, S. Horiuchi, S. Horie, *J. Mater. Chem.* 2010, **20**, 4784–4791; K. Ichimura, *Chem. Lett.* 2010, **39**, 614–615.
- (11) G. Kaupp, *CrystEngComm* 2009, **11**, 388–403; D. Braga, F. Grepioni, *Angew. Chem. Int. Ed.* 2004, **43**, 4002–4011; A. L. Garay, A. Pichon, S. L. James, *Chem. Soc. Rev.* 2007, **36**, 846–855; T. Friščić, E. Meštrović, D. Š. Šamec, B. Kaitner, L. Fábián, *Chem. Eur. J.* 2009, **15**, 12644–12652; K. Tanaka,; F. Toda, *Chem. Rev.* 2000, **100**, 1025–1074; D. R. Weyna, T. Shattock, P. Vishweshwar, M. Zaworotko, *Cryst. Growth Des.* 2009, **9**, 1106–1123.
- (12) T. Inabe, H. Tajima, *Chem. Rev.* 2004, **104**, 5503–5534; C. J. Schramm, D. R. Stojakovic, B. M. Hoffman, T. J. Marks, *Science* 1978, **200**, 47–48
- (13) C. J. Schramm, R. P. Scaringe, D. R. Stojakovic, B. M. Hoffman, J. A. Ibers, T. J. Marks, *J. Am. Chem. Soc.* 1980, **102**, 6702–6713
- (14) M. Y. Ogawa, J. Martinsen, S. M. Palmer, J. L. Stanton, J. Tanaka, R. L. Greene, B. M. Hoffman, J. A. Ibers, *J. Am. Chem. Soc.* 1987, **109**, 1115–1121.
- (15) G. Maggioni, S. Carturan, M. Tonezzer, M. Bonafini, A. Vomiero, A. Quaranta, C. Maurizio, F. Giannici, A. Scandurra, F. D’Acapito, G. D. Mea, O. Puglisi, *Chem. Mater.* 2006, **18**, 4195–4204; J. H. Sharp, M. Abkowitz, *J. Phys. Chem.* 1973, **77**, 477–481.
- (16) K. Ichimura, A. Funabiki, K. Aoki, H. Akiyama, *Langmuir* 2008, **24**, 6470–6479.
- (17) A. Funabiki, H. Sugiyama, T. Mochida, K. Ichimura, T. Okubo, K. Furukawa, T. Nakamura, unpublished work.
- (18) S. Hara, H. Tanaka, T. Kawamoto, M. Tokumoto, M. Yamada,; A. Gotoh, H. Uchida, M. Kurihara, M. Sakamoto, *Jpn. J. Appl. Phys.* 2007, **46**, L945–L947; H. Shiozaki, T. Kawamoto,

H. Tanaka, S. Hara, M. Tokumoto, A. Gotoh, T. Satoh, M. Ishizaki, M. Kurihara, M. Sakamoto, *Jpn. J. Appl. Phys.* 2008, **47**, 1242–1244; S. Hara, H. Shiozaki, A. Omura, H. Tanaka, T. Kawamoto, M. Tokumoto, M. Yamada, A. Gotoh, M. Kurihara, M. Sakamoto, *Appl. Phys. Express*, 2008, **1**, 104002-1–3.

(19) Electronic Supplementary Information (ESI) available: FTIR spectra of CuPc before and after milling with silica nanoparticles (Fig. S1), SEM images of CuPc–silica hybrid nanoparticles and [CuPc]I nanorods (Figs. S2 and S3), an EDX spectrum of [NiPc]I nanorods (Fig. S4), and an electron diffraction image of [NiPc]I nanorods (Fig. S5).

## Figure Caption

**Fig. 1.** Chemical formula of metal phthalocyanine iodide.

**Fig. 2.** Powder XRD patterns of (a) NiPc (bulk powders,  $\beta$ -form), (b) as-prepared NiPc–silica hybrid nanoparticles, (c) as-prepared CuPc–silica hybrid nanoparticles and (d) CuPc–silica hybrid nanoparticles after annealing at 250 °C.

**Fig. 3.** Powder XRD patterns of (a) [NiPc]I–silica nanocomposite prepared under dry conditions before and (b) after washing with hexane, (c) [NiPc]I–silica nanocomposite prepared under wet conditions and (d) a simulated pattern of [NiPc]I.<sup>13</sup>

**Fig. 4.** TEM images of [NiPc]I–silica nanocomposites prepared under dry conditions followed by washing with hexane. Figure b shows an enlarged image of a [NiPc]I nanorod.

**Fig. 5.** SEM images of (a) bundled and (b) isolated [NiPc]I–silica nanocomposites prepared under wet conditions.

**Fig. 6.** TEM elemental mapping images of the [NiPc]I–silica nanocomposite prepared under dry conditions. (a) [NiPc]I nanorods, and images corresponding to the mapping of (b) carbon, (c) nickel, (d) iodine, (e) silicone and (f) oxygen.

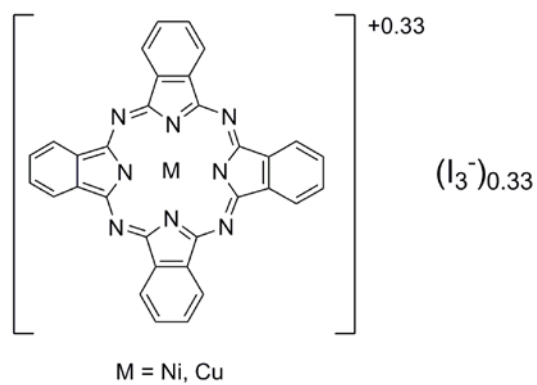


**Fig. 1.**

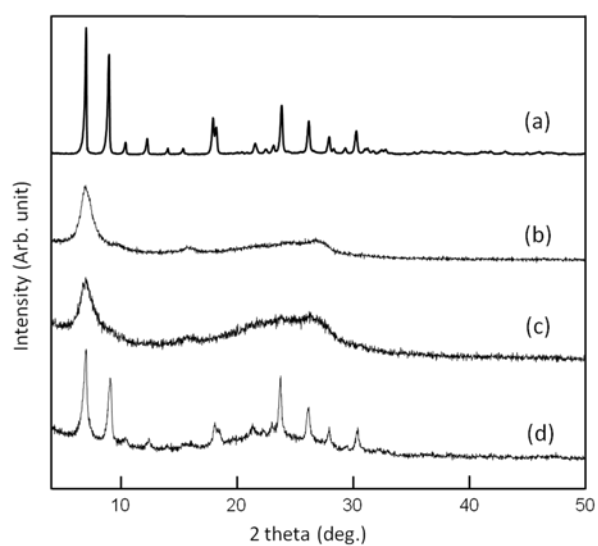


**Fig. 2.**

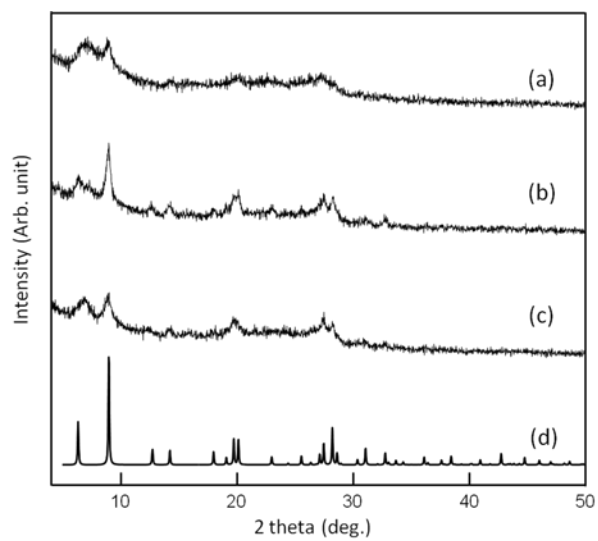


**Fig. 3.**



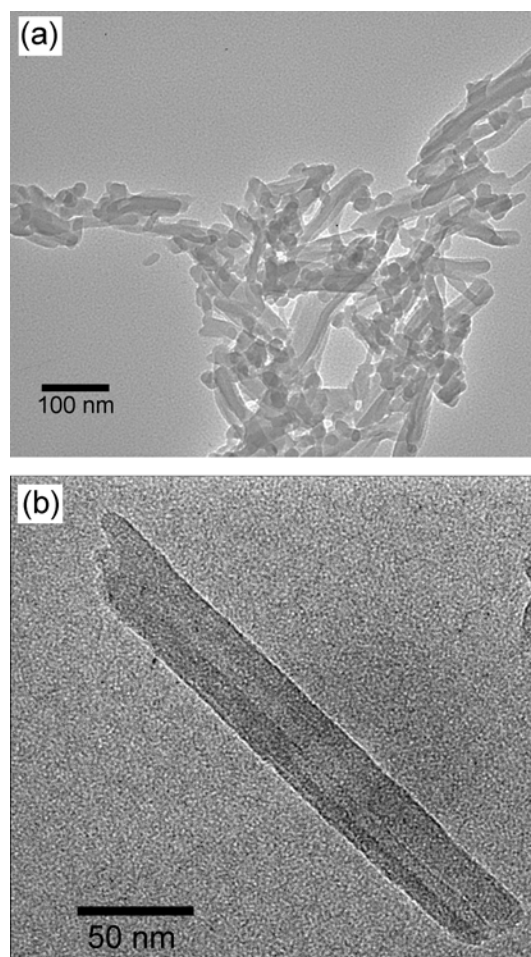


**Fig. 4.**

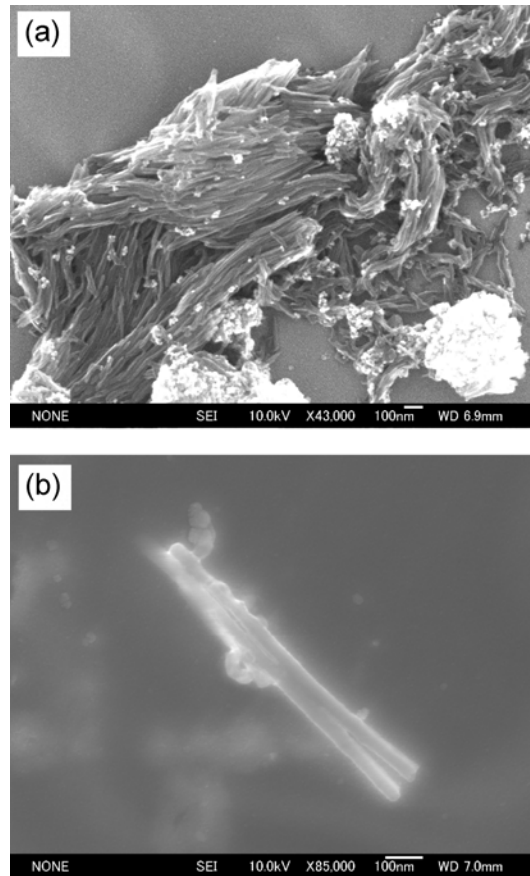


**Fig. 5.**

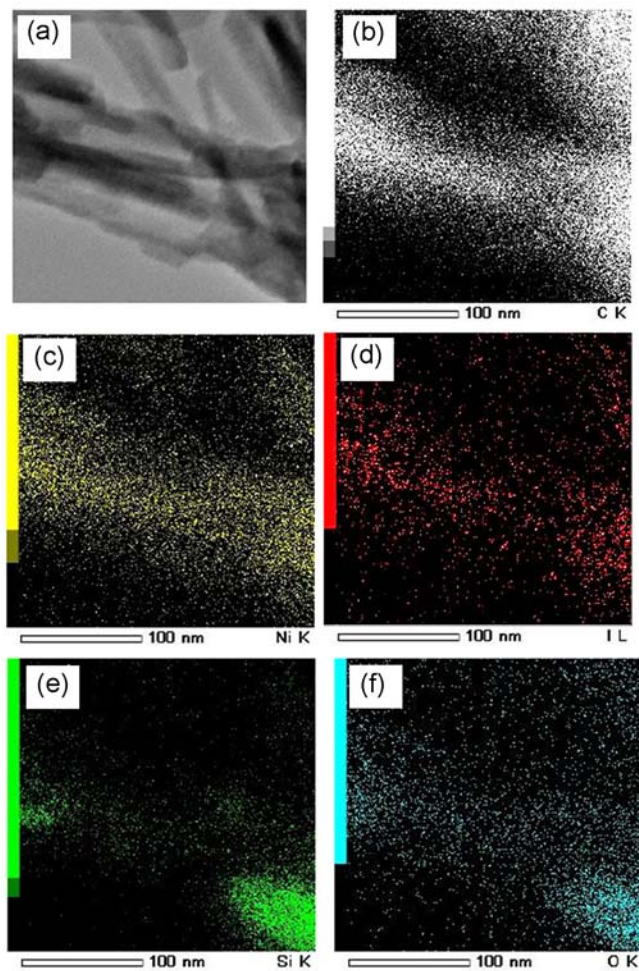


**Fig. 6.**

## Supporting Information

### Nanosized charge-transfer salts of metal phthalocyanine iodides ([MPc]I) produced by direct reaction of MPc–Silica hybrid nanoparticles with iodine

Akira Funabiki,<sup>a</sup> Tomoyuki Mochida,<sup>\*,a</sup> Hiroyuki Hasegawa,<sup>b,c</sup> Kunihiro Ichimura,<sup>d</sup> and Seiji Kimura<sup>e</sup>

<sup>a</sup>Kobe University, <sup>b</sup>Kobe Advanced ICT Research Center, National Institute of Information and Communications Technology, <sup>c</sup>PRESTO, <sup>d</sup>Toho University, <sup>e</sup>The University of Electro-Communications

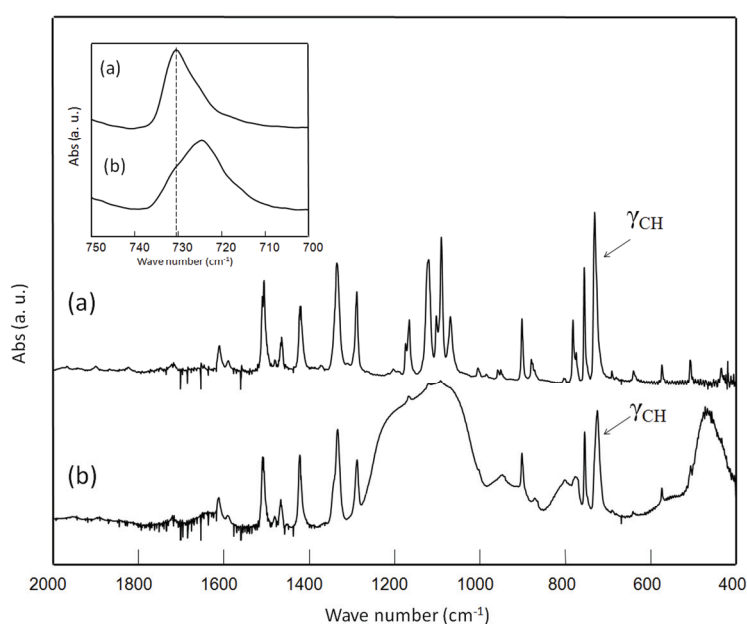


**Figure S1.** FTIR spectra of (a) CuPc bulk powder and (b) CuPc–silica hybrid nanoparticles.

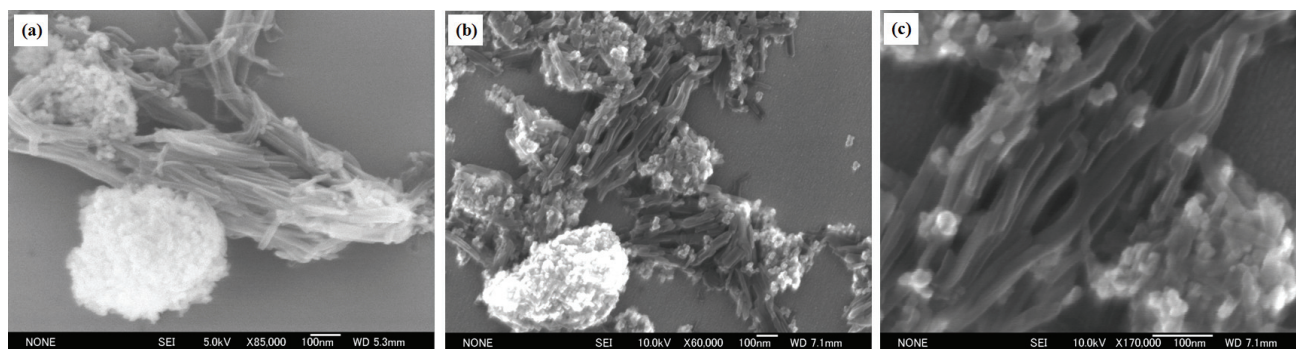


**Figure S2.** SEM images of [CuPc]I-silica nanocomposites prepared under (a) dry and (b, c) wet conditions.

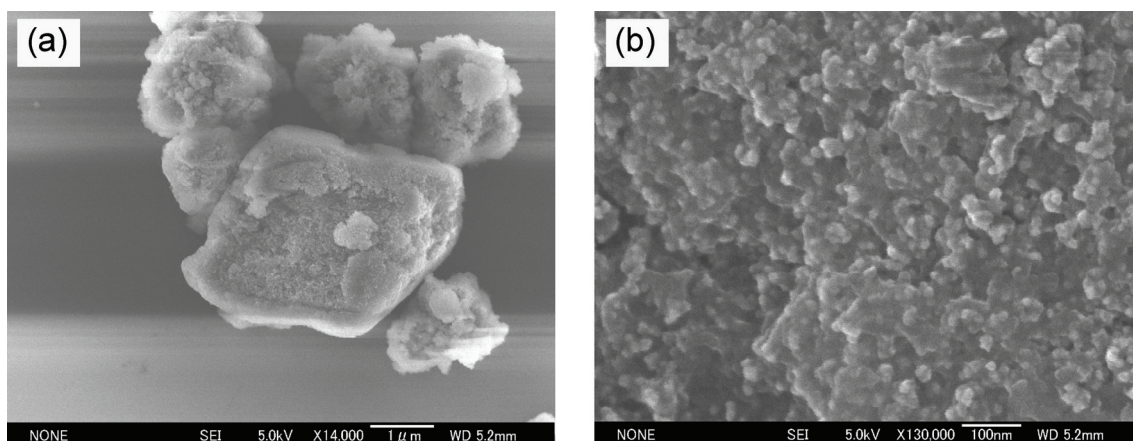


**Figure S3.** SEM images of CuPc-silica hybrid nanoparticles before reaction with iodine.

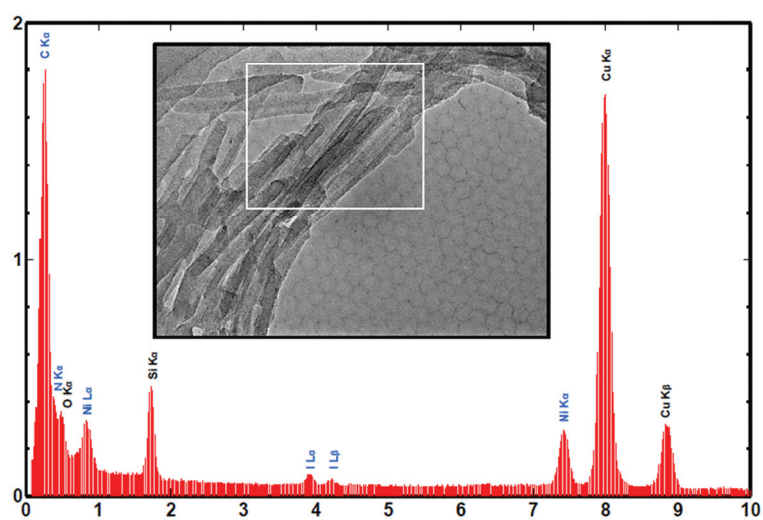


**Figure S4.** A TEM image and an EDX spectrum of the [NiPc]I nanorods in the composite prepared under dry conditions. The spectrum was obtained from the framed part in the TEM image.

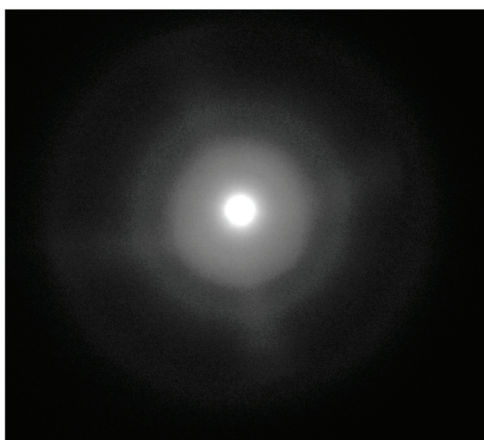


**Figure S5.** An electron diffraction pattern of [NiPc]I nanorods obtained under dry conditions.